Heliyon 5 (2019) e01841

Contents lists available at ScienceDirect

Heliyon

journal homepage: www.heliyon.com

Detailed structural assessment of healthy interventricular septum in the presence of remodeling infarct in the free wall – A finite element model

Fulufhelo Nemavhola *

Department of Mechanical and Industrial Engineering, School of Engineering, College of Science, Engineering and Technology, University of South Africa, Florida, South Africa

ARTICLE INFO

Keywords:
Biomedical engineering
Bioengineering
Mechanics
Finite element modelling
Bi-ventricular heart model
Computational mechanics
Myocardial stress
Myocardial strain

ABSTRACT

Purpose: Computational modelling may improve the fundamental understanding of various mechanisms of diseases more particularly related to clinical challenges. In this study the effect of remodeling infarct presence in the left ventricle on the interventricular septal wall is studied using the finite element methods.

Methods: In this study, two rat heart (one model with healthy myocardium and one model with remodeling free wall and healthy septal wall) with magnetic resonance imaging data was gathered to reconstruct three-dimensional (3D) rat heart models. 3D data points from Segment® were imported into SolidEdge® for creation of 3D rat heart models. Abaqus® was used for finite element modeling.

Results: The strain in the healthy interventricular septum of the infarcted left ventricle wall increased when compared to the healthy interventricular septum in the healthy left ventricle. Similarly, the average stress in the healthy left ventricle was observed to have increased on the healthy the interventricular septum where the free wall is subjected to remodeling infarct. When comparing the infarcted models to the healthy model, it was found that the average strain had greatly increased by up to 50.0 %.

Conclusions: The remodeling infarct in the left ventricle has an impact on the healthy interventricular septal wall. Even though the interventricular septal wall was modelled as healthy, it was observed that it has undergone considerable changes in stresses and strains in circumferential and longitudinal direction. The observed changes in myocardial stresses and strains may result in poor global functioning of the heart.

1. Introduction

Myocardial infarction (MI) is caused by the blockage of the coronary artery which may further cause the imbalance between oxygen supply and myocardial demand [1]. Within few minutes after the blockage of the coronary artery, the contraction function on the myocardium is immediately compromised and shortly within few hours the myocytes begin to die [2]. After few weeks the myocytes die and gradually replaced by the collagen scar tissue formed by fibroblasts. These changes have serious implication as they begin to compromise the mechanical response of the myocardium [3]. During the progression of healing infarct in the myocardium, the depression of global function of the heart sets in. This may lead to LV remodelling which may ultimately lead to infarct rapture or heart failure [4]. It has been proven that computational modelling may improve the fundamental understanding of various mechanisms of diseases more particularly related to clinical challenges [5]. Computational modelling requires the accurate imaging data and accurate boundary conditions to simulate that real situation by utilising complex mathematical equations. Computational modelling in heart diseases plays an important role the development of new devices to assist patients suffering from various diseases [6]. In addition, patient-specific computational simulation may lead to specific outcomes that may assist in the development of therapeutic solutions [7]. Around half of Americans experience myocardial infarction each year. Moreover, the clinical cardiology tends to concentrate on the administration of healing or healed infarcts [8]. Hence, much advance has been accomplished by pharmacological treatments to counteract or restrict left ventricle remodelling which can prevent advancement to fully dilated heart failure [9, 10]. While this has been accomplished by for the most part *ex-vivo* experiments and MRI studies [11, 12], there is a need to additionally create and develop the computational models [13, 14] which will additionally aid in the understanding how infarcted tissue behaves under different conditions.

Cardiovascular biomechanics relies on upon different heart stages and might be mutilated by an assortment of cardiovascular conditions.

* Corresponding author.
E-mail address: masitfj@unisa.ac.za.

https://doi.org/10.1016/j.heliyon.2019.e01841
Received 10 February 2019; Received in revised form 9 April 2019; Accepted 24 May 2019

Even though the strain distribution can be measured experimentally and clinically by MRI, computational models can be utilized to quantify the local wall stresses and strains. In addition to accurate geometries, constitutive laws that reflect the non-linear elastic behaviour and boundary conditions that mimic the physiological accuracy become important. Magnetic resonance imaging (MRI) information were utilized to make the geometry of the bi-ventricular model of non-infarcted and infarcted rat heart. The general-purpose software Abaqus® was used to simulate models subjected to boundary conditions. Transversely isotropic strain energy function (Fung model) was used to model the diastolic filling.

In the rat heart, most studies have determined that the remodeling of left ventricle occurs in the period between 14 and 28 days. In the process of remodeling ventricle, the structure losses its integrity by decoupling collagen content [9]. The increase in collagen content in the ventricular wall may contribute to the increase of stiffness in the remodeling infarct. During this stage the infarct ensures that the infarcted region loses its structural integrity and then remodel. Initially, the may show signs of shrinking first. The shrinkage is understood to also affect the global functioning of the heart because of lessening of ventricular volume.

The fiber orientation in the infarct region is understood to be affected. The effect and change of fiber orientation in the affected area is based on change of collagen content. The change in collagen content and fiber direction may also contribution to the mechanical strength and behavior of the infarcted myocardium [15]. Because of changes in the structural integrity of the myocardium, the cavity dilation occurs and the compromise in global functioning of the heart also surfaced. To capture the image of the rat heart, MRI has been used in clinical applications for several decade [16].

It is reported that presence of fibrotic infarction in the left ventricle (LV) has adverse effect on the septal wall hence poor functioning of the heart [17]. This is a follow-up paper looking at the effect of remodelling infarct on the septal wall in the presence of remodelling infarction. The current study looks at the effect of remodelling infarct whereas the previous study observed on the effect of the fibrotic infarct on the healthy septal. In this case, the septal wall is not exposed to infarct injury but only the LV. The aim is to assess whether the presence of infarct on the free wall has a significant effect on the septal wall during passive filling. This has been achieved by looking at the 3D rat heart model of the healthy and the infarcted heart model.

2. Materials and methods

In this study the first step was to obtained magnetic resonance imaging (MRI) scans. The scans obtained were obtained using a MAGNETOM Allegra 3T MRI scanner (Siemens, Erlangen, Germany) at the University of Cape Town, Cape Town, South Africa. Ethical clearance was obtained from the University of Cape Town regarding the MRI experimental studies. The bore of the normal 3T MRI are larger and not suitable for small animal imaging, hence, the small polarized circular coil of inner diameter of 70 mm was used to receive and transmit the signal [18]. The MRI data was processed and imported to Segment [19]. In this case both left and right ventricles were segmented manually to ensure that good accuracy is achieve. Several stakes of imagines were obtained from the MAGNETOM Allegra 3T MRI. The MRI data was segmented from the short-axis of the rat heart. The segmented data was there exported to Segment® software designed for heart imagine segmentation [19]. Fig. 1(a) shows the 3D segmented rat heart model with visible remodeling infarct in the LV. The segmented data was then exported to Microsoft Excel in x,y,z coordinates. The SolidEdge® TS5 was then used to produce 3D CAD rat heart models for finite element modeling (Siemens PLM Software, Inc.) from the x,y,z data from Segment® software as shown in Fig. 1 (b and c). Biventricular FE models of both the healthy and remodelling models were created using the animal-specific surface geometries from MRI data and the mesh were generated using (Abaqus® FEA (D S Simulia. ©Dassault Systemes, Providence, USA, 2007). 10-node tetrahedral elements were used to mesh the ventricles with approximately 8510 as shown in Fig. 2 (b). The values of material parameters used in this model are shown in Table 1 [20]. These parameters were changes during validation processes and were amended as shown in Table 1. The transmural mesh density was adjusted until the ventricular volume changed by 5% for a given load. It was found that three elements are sufficient for accurate ventricular volume calculations and computational efficiency [21]. During the heart cycle of contraction and relaxation, the fibre arrangement plays a vital role in the functioning of the heart [22]. Furthermore, fibre arrangement in the heart wall ensures that electrical signals are used for accurate contraction of the heart [23]. RTO model the myofibre of the heart, myofibre angles a custom inhouse ORIENT Abaqus© subroutine was used to assign the fibre angle at each node. This fibre distribution was used throughout the entire healthy rat heart model including left ventricle (LV), the septum, and RV free wall. Fiber angles at the infarcted regions were not assigned [9]. Ventricular remodelling and tissue healing after myocardial infarction are dynamic and simultaneous processes [24]. To apply the boundary conditions, at the basal position, the nodes were constrained in both the circumferential and longitudinal directions.

To mimic the heart movement at the base, all elements were left to have free movement. The inner endocardial pressures of 2.4 kPa and 0.08 kPa were assigned on the cavities of left ventricle and right ventricle, respectively (See Fig. 2a). User-defined material subroutine in the explicit FE solver of Abaqus® [25] was used to simulate the nearly incompressible, transversely isotropic and hyperelastic constitutive models for passive [20]. The healthy and infarcted material were both modelled as passive material using the Fung model [26]. The Fung model is represented by the strain energergy function as follows:

$$W = \frac{1}{2}C\left(e^{Q} - 1\right)$$

Where:

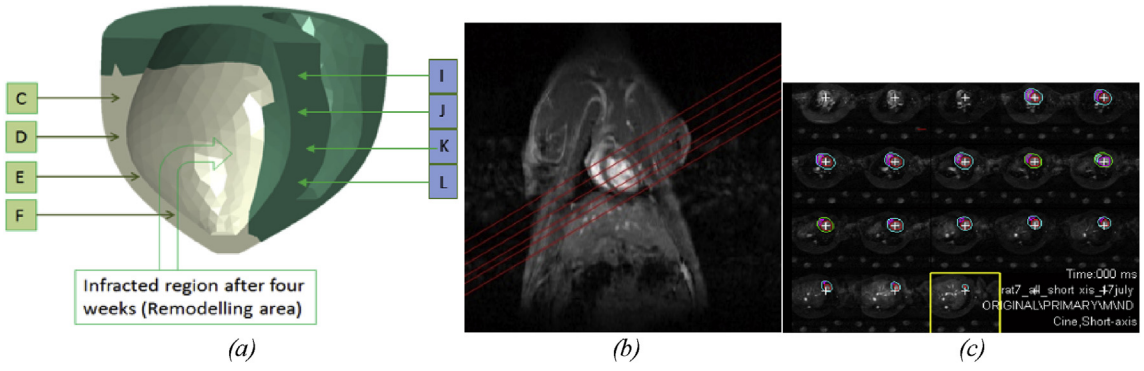

Fig. 1. (a) Considered transmural regions on the septal wall, (b) MRI image of long-axis segmentation of the rat heart and (c) Short axis segmentation of rat heart.

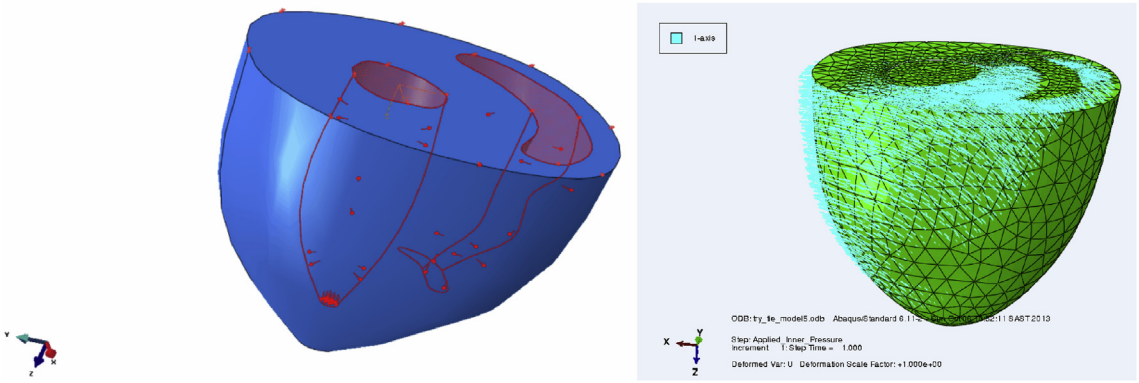

(a) (b)

Fig. 2. 3D rat heart model created by segmenting the MRI data (a) Endocardial pressure applied on the RV and LV of the 3D rat heart model to mimic passive filling. (b) 10-node tetrahedral quadratic elements applied on the 3D rat heart model.

Table 1
Fung model material parameters applied on the LV and RV 3D rat heart model to mimic the mechanical behaviour of passive myocardium [20].This Table shows the material properties used in the Fung model for modelling the healthy tissue of the rat heart.

Parameter	Fibre strain coefficient	Cross-fibre strain coefficient	Shear strain coefficient	Stress scaling factor
Constants	b_1	b_2	b_3	C (MPa)
Value	9.2	3	3.7	0.002

$$Q = \left[b_f E_{11}^2 + b_t\left(E_{22}^2 + E_{33}^2 + E_{23}^2 + E_{32}^2\right) + b_{fs}\left(E_{12}^2 + E_{21}^2 + E_{13}^2 + E_{31}^2\right)\right]$$

Where E_{11}, E_{22} and E_{33} are the fibre, cross-fibre and radial strains, respectively. E_{23}, E_{12} and E_{13} are shear strains, transverse plane strains and the shear strains in the fibre-cross-fibre and fibre-radial planes, respectively. C is regarded the the material constant of the Fung model. To model the stiffness of the infarct in the left ventricle, the C was assigned value of ten times the value of the healthy myocardium. Values for the material constants b_1, b_2 and b_3 were chosen as 9.2, 3.0 and 3.7, respectively, based on the previous studies of rat myocardium [20]. The rat heart 3D model was validated by adjusting the material constant C until the match of left ventricle and right ventricle end-diastole volumes matched with that of the MRI data (See Table 2). It should be noted that the myocardial material properties [27] have been used in previous biventricular FE simulations of the rat heart.

3. Results

Passive filling was modelled by applying inner pressure on the free wall and septal wall. The same magnitude of pressure was applied in healthy (healthy free wall and septal wall) (HFHS) model and infarcted (infarcted free wall and healthy septal wall) (IFHF) model. The average stresses and strains in the radial, circumferential and longitudinal directions were calculated using selected regions/paths as shown in Fig. 1 (a). The stresses and strains in the radial, circumferential and longitudinal directions are presented in Figs. 3 and 4. Figs. 3 and 4 show a contour plot in the x-axis (mid-heart) and in the long-axis, respectively.

The graphic shows the stresses and strains of biventricular model of rat heart of both the HFHS and IFHF models. The radial, circumferential and longitudinal stresses and strains at epicardium, mid-wall and endocardium of IFHS and HFHS models are presented in Figs. 5 and 6, respectively. In order to understand the effect of remodelling heart on the mechanics of septal wall, the average stresses and strains were plotted for both IFHF and HFHF models in Figs. 5 and 6. Generally, for both the IFHF and HFHS models, the greatest radial stress is observed in the endocardium, the followed by the mid-wall and the smallest radial stress magnitude was observed in the epicardium (see Fig. 6).

Similarly, in both IFHF (remodelling infarcted rat heart) and HFHS (healthy rat heart) models, the highest circumferential stress was found in the endocardium. The smallest circumferential stress was observed in

Table 2
Fung model material constant c applied for the healthy and remodelling (four-week infarcted) models. The collagen changes in the infarcted myocardium stiffens the mechanical behaviour of the materials. To account for the effect of material behaviour change the scalling factor c is changed to 0.02 MPa in the infarcted myocardium.

	C - Material constant Healthy heart model	C - Material constant Remodelling Infarcted model
Healthy model	0.002 MPa	n/a
Four-week	0.002 MPa	0.02 MPa

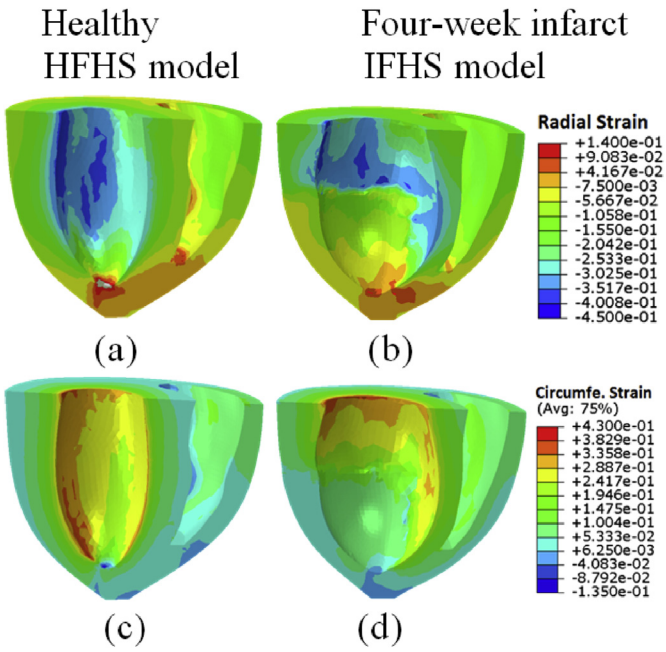

Fig. 3. Contour plots of end-diastolic strain in long axis of the 3D rat heart model of the healthy and remodelling (four-week model) heart models. (a)–(b): Radial strain and (c)–(d): Circumferential strain.

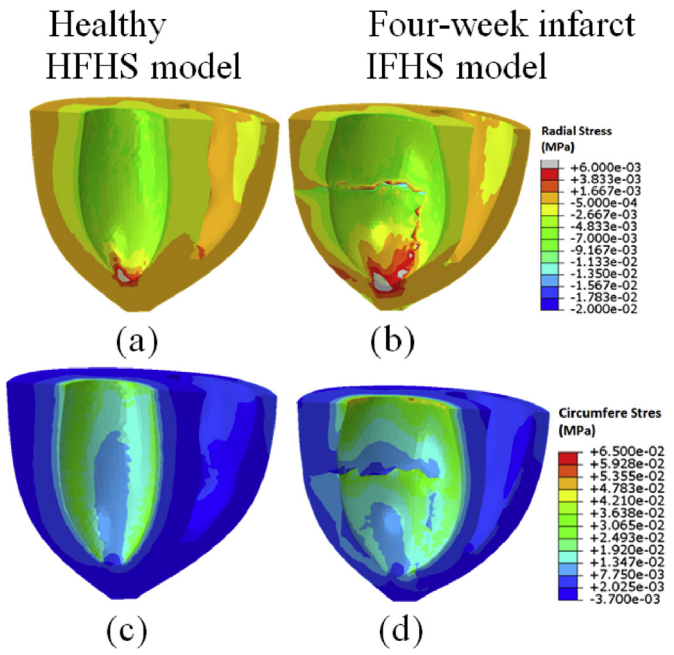

Fig. 4. Contour plots of end-diastolic stress in long axis of the 3D rat heart model of the healthy and remodelling (four-week model) heart models. (a)–(b): Radial stress and (c)–(d): Circumferential stress.

the epicardium (see Fig. 5. As shown in Fig. 5, the highest radial, circumferential and longitudinal strain in both IFHF and HFHS model were found in the endocardium. Generally, as shown in Fig. 5, the lowest radial, circumferential and longitudinal strain were recorded in the epicardium for both IFHF and HFHS models. The average stresses and strains for IFHS and HFHS models are calculated by considering region I, J, K and L in the septal wall. The average stress and strain are shown in Figs. 5 and 6, respectively. Validation of MRI data and the reconstructed 3D computational models are shown in Table 3.

4. Discussion

The computational modelling of the cardiovascular system has been further improved by the recent improvement of computer technology [28, 29]. Electrophysiological and mechanical response of the healthy and infarcted hearts may be developed by using the virtual heart models [30]. For decades now, several researchers have studied the effect of myocardial infarction on the performance of the heart [31]. The behaviour of wall mechanics due to infarct healing and post infarct ventricular remodelling were also studied [20, 32, 33, 34, 35, 36, 37, 38].

The effect of overload RV interventricular Septum (here referred as septal wall or mid-wall) have been studied intensively [29]. The current study has however also assessed in detail the changes in wall mechanics of the septal wall in presence of an infarct in the LV free wall. The current study differs with [29] as the main approach was to investigate the effect of remodelling infarct present on the LV on the septal wall. However, myocardial fibre stress in healthy control increased due to overloaded RV. In this study, it was found that both radial and circumferential stresses in the interventricular septum increased to due remodelling infarct present in the LV. As pointed out before, the septal wall is not exposed to infarct injury and healing but remains healthy and functional, i.e. contractile while the LV infarct region and LV undergoes the stages of infarct healing and ventricular remodelling. Substantial changes in strains and stresses have been observed in the septal wall between the healthy heart and the infarcted heart.

The study of the effect of fibrotic infarct on the healthy interventricular septum during passive filling clearly indicates that the infarct may compromise the global function if the heart [17]. This current study however looks at the effect of remodelling infarct on the heathy septal wall. It is now shown that both fibrotic infarct (as previously reported [17]) and remodelling infarct (in this current study) has an impact on the effectiveness and efficiency of the septal wall hence the global function of the heart. As the scar tissue stiffens, the average strain in all directions decreased. Hence, the average strain in the healthy tissue was found to be higher that of the scar tissue (see Figs. 5 and 6). In the process of remodeling ventricle, the structure losses its integrity by decoupling collagen content [9]. The increase in collagen content in the ventricular wall may contribute to the increase of stiffness in the remodeling infarct [15, 39]. During the process of infarct healing, the collagen structures changes and new deposits develops in the remodelling infarct. Immidiately after structural changes of the collagen, the mechanical behaviour of the infarct changes. Additionally, the collagen fibers also emerges form the epicardium to endocardium. During this stage, the stiffness of the infarct increases [39].

The effect of myocardial infarction has been studied by various researchers [40, 41]. Various therapies have been suggested to prevent further progression of the condition [41, 42, 43]. The presented results show that the infarct size has major influence on the average strain in radial, circumferential and longitudinal directions. It is clear that the average strain in the septal wall is greatly influenced by the size of the infarcted tissue in the free wall (see Fig. 5). Surprisingly, the infarct size on the free wall does not restrain the septal wall; instead it allows the septal wall to have greater movement. When comparing the infarcted models to the healthy model, it was found that the average strain has greatly has increased by up to 50.0 %. Fascinatingly, in the four-week model (which has the highest infarct size), the average strain has risen up to 50.0 %. Generally, it was observed that the average stresses (radial, circumferential and longitudinal) in the septal wall in the IFHS model,

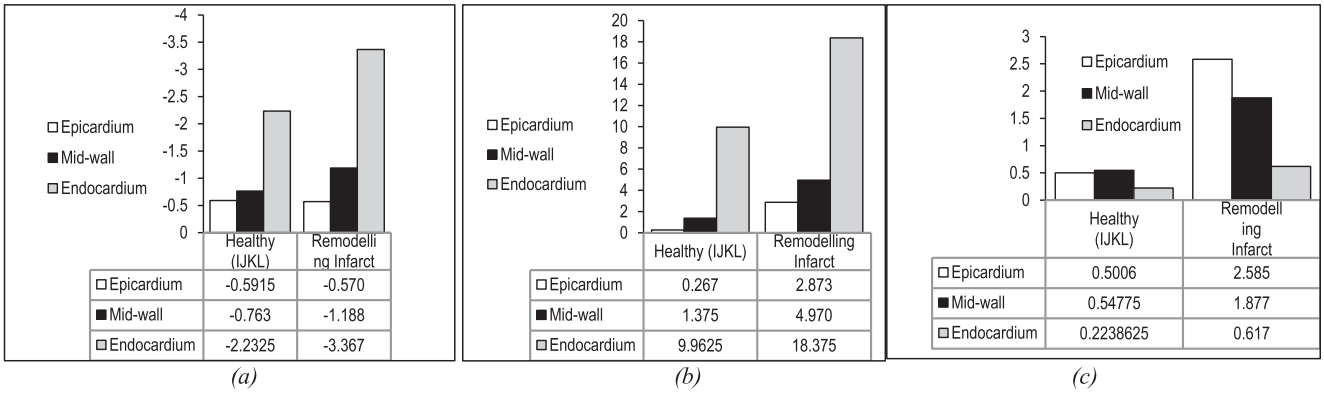

Fig. 5. End-diastolic stress for healthy (HFHS model) and four-week (IFHS model) remodelling infarct models. (a) Average radial (b), circumferential and (c) longitudinal stress at paths I, J, K and L. All units in kPa.

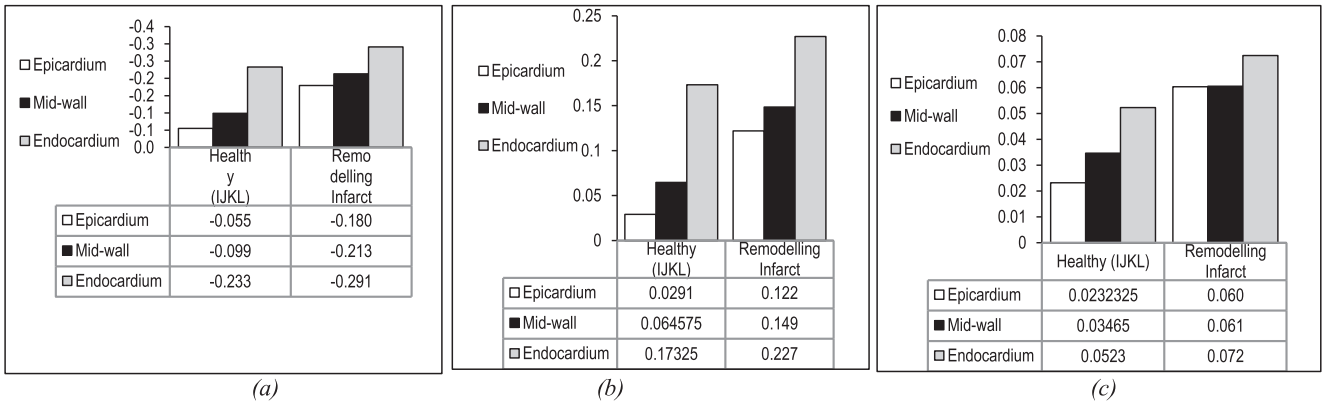

Fig. 6. End-diastolic strain for healthy (HFHS model) and four-week (IFHS model) remodelling infarct models. (a) Average radial (b), circumferential and (c) longitudinal stress at paths I, J, K and L. All units in kPa.

Table 3
Comparison of reconstructed and MRI heart geometries - cavity and wall volumes and cavity area of LV for healthy and four-week infarct models and Comparison of error for MRI data and 3D reconstructed heart geometries.

Comparison of reconstructed heart geometries - cavity and wall volumes and cavity area of LV			
	Cavity Volume (μL) (LV only)	Cavity Area (mm2) (LV only)	Wall Volume (μL) (LV plus RV)
Healthy	73.00	108.7	763.9
Four-week infarct	186.2	166.5	656.52
Comparison of MRI heart geometries - cavity and wall volumes and cavity area of LV			
Healthy	73.56	106.23	765.67
Four-week infarct	188.62	168.54	650.52
Comparison of error 3D reconstructed heart geometries and MRI data			
Healthy	0.81 %	2.36 %	0.24 %
Four-week infarct	1.30 %	1.22 %	0.92 %

have higher magnitude when compared to the septal wall in the HFHS model) (see Fig. 5).

The MRI data was used to develop the biventricular rat heart model. To simulate the end-diastolic pressure, the constant pressure was applied on the ventricular cavity of the left ventricle and right ventricle. Because of the stiffening of scar due to the infarct, the free wall becomes subjected to less strain. The less strain or movement of the free wall contributed to the high strain of the interventricular septal wall. This is because the myocardial energy if forced to absorb the energy impact of the high stiffness of the free wall.

It is concluded that after infarction, the septal wall works much harder than it used to do due to the restrain movement on the free wall. These findings have practical implications as when the free wall stretches beyond its limit, the wall rapturing may occur. Since infarct rigidity and collagen content increment in parallel among the fibrotic stage, it appears glaringly evident that collagen content is one essential determinant of the mechanical properties of the healing infarct amid this stage.

In this study, the infarcted tissue has been found to be stretching in circumferential and longitudinal directions. Infarct extension is a generally perceived component of post-infarction remodelling that relates to more abysmal clinical results and has been focused by various developed therapies, treatments and rehabilitations. Utilizing a finite element model, we exhibit that the stability between scar hardening because of collagen aggregation and increased wall stresses because of infarct dilution can deliver either extension or compaction in the pressurized heart and that loaded dimensions are significantly more delicate to changes in thickness than in stiffness or hardening.

5. Conclusions

The 3D biventricular rat heart model was developed. Fung model was utilised in assessing the effect of remodelling infarct present on the left ventricle in the healthy interventricular septal wall. The stresses and strains in the circumferential and longitudinal directions were assessed on healthy and remodelling heart model at end-systole. In this study, the interventricular septum is considered heathy by the left ventricle (free wall) is subjected to remodelling infarct. The remodelling infarct in the left ventricle has an impact on the healthy interventricular septal wall. Even though the interventricular septal wall was modelled as healthy, it was observed that it has undergone considerable changes in stresses and strains in circumferential and longitudinal direction. The observed mechanism may result in poor global functioning of the heart. Finite Element Modelling (FEM) tool is efficient in the understanding of various mechanisms of cardiovascular diseases.

Declarations

Author contribution statement

F. Nemavhola: Conceived and designed the experiments; Performed the experiments; Analyzed and interpreted the data; Contributed reagents, materials, analysis tools or data; Wrote the paper.

Funding statement

The author would like to acknowledge the National Research Foundation of South Africa, the University of SouthAfrica and University of Cape Town for their contribution.

Competing interest statement

The authors declare no conflict of interest.

Additional information

No additional information is available for this paper.

Acknowledgements

The authors thank Dr. Mohamed Saleh, Prof E Meintjes, Dr. EM Alhamud A and Dr. BS Spottiswoode for the development of GE sequence (fast low angle shot (FLASH) used to obtain cine cardiac images for functional and structural assessment and Dr. S–K Sharp for handling the

animals at the University of Cape Town. Doctoral supervisors, Prof T Franz and Prof Neil Davis are also acknowledged from the University of Cape Town.

References

[1] A. Moore, et al., Acute myocardial infarct, Radiol. Clin. 57 (1) (2019) 45–55.
[2] R. Tennant, C.J. Wiggers, The effect of coronary occlusion on myocardial contraction, Am. J. Physiol. Leg. Content 112 (2) (1935) 351–361.
[3] C. Connelly, et al., Movement of necrotic wavefront after coronary artery occlusion in rabbit, Am. J. Physiol. Heart Circ. Physiol. 243 (5) (1982) H682–H690.
[4] S.A. Clarke, W.J. Richardson, J.W. Holmes, Modifying the mechanics of healing infarcts: is better the enemy of good? J. Mol. Cell. Cardiol. 93 (2016) 115–124.
[5] H. Yu, et al., Patient-specific in vivo right ventricle material parameter estimation for patients with tetralogy of Fallot using MRI-based models with different zero-load diastole and systole morphologies, Int. J. Cardiol. 276 (2019) 93–99.
[6] G. Biglino, et al., Computational modelling for congenital heart disease: how far are we from clinical translation? Heart 103 (2) (2017) 98–103.
[7] T. Conover, et al., An interactive simulation tool for patient-specific clinical decision support in single-ventricle physiology, J. Thorac. Cardiovasc. Surg. 155 (2) (2018) 712–721.
[8] A. Gulhane, H. Litt, Acute coronary and acute aortic syndromes, Radiol. Clin. 57 (1) (2019) 25–44.
[9] J.W. Holmes, T.K. Borg, J.W. Covell, Structure and mechanics of healing myocardial infarcts, Annu. Rev. Biomed. Eng. 7 (2005) 223–253.
[10] W. Kosmala, et al., Comparison of the diastolic stress test with a combined resting echocardiography and biomarker approach to patients with exertional dyspnea: diagnostic and prognostic implications, JACC (J. Am. Coll. Cardiol.): Cardiovasc. Imaging 12 (5) (2019) 771–780.
[11] W. Kosmala, M. Przewlocka-Kosmala, T.H. Marwick, Association of active and passive components of LV diastolic filling with exercise intolerance in heart failure with preserved ejection fraction: mechanistic insights from spironolactone response, JACC (J. Am. Coll. Cardiol.): Cardiovasc. Imaging 12 (5) (2019) 784–794.
[12] G. Buonincontri, et al., PET/MRI assessment of the infarcted mouse heart, Nucl. Instrum. Methods Phys. Res. Sect. A Accel. Spectrom. Detect. Assoc. Equip. 734 (2014) 152–155.
[13] R.R. Rama, S. Skatulla, Towards real-time modelling of passive and active behaviour of the human heart using PODI-based model reduction, Comput. Struct. (2018) [In Press, Corrected Proof].
[14] R.R. Rama, S. Skatulla, Towards real-time cardiac mechanics modelling with patient-specific heart anatomies, Comput. Methods Appl. Mech. Eng. 328 (2018) 47–74.
[15] G.M. Fomovsky, A.D. Rouillard, J.W. Holmes, Regional mechanics determine collagen fiber structure in healing myocardial infarcts, J. Mol. Cell. Cardiol. 52 (5) (2012) 1083–1090.
[16] G.J. Heatlie, K. Pointon, Cardiac magnetic resonance imaging, Postgrad. Med. 80 (939) (2004) 19–22.
[17] F. Nemavhola, Fibrotic infarction on the LV free wall may alter the mechanics of healthy septal wall during passive filling, Bio Med. Mater. Eng. 28 (6) (2017) 579–599.
[18] M.G. Saleh, et al., Long-Term left ventricular remodelling in rat model of nonreperfused myocardial infarction: sequential MR imaging using a 3T clinical scanner, J. Biomed. Biotechnol. (2012) 10.
[19] E. Heiberg, et al., Design and validation of Segment-freely available software for cardiovascular image analysis, BMC Med. Imaging 10 (1) (2010) 1.
[20] J.H. Omens, D.A. MacKenna, A.D. McCulloch, Measurement of strain and analysis of stress in resting rat left ventricular myocardium, J. Biomech. 26 (6) (1993) 665–676.
[21] N. Sun, et al., Computational modeling of LDL and albumin transport in an in vivo CT image-based human right coronary artery, J. Biomech. Eng. 131 (2) (2009) 021003–021009.
[22] William J. Richardson, Jeffrey W. Holmes, Emergence of collagen orientation heterogeneity in healing infarcts and an agent-based model, Biophys. J. 110 (10) (2016) 2266–2277.
[23] A.D. Rouillard, J.W. Holmes, Coupled agent-based and finite-element models for predicting scar structure following myocardial infarction, Prog. Biophys. Mol. Biol. 115 (2) (2014) 235–243.
[24] S.D. Zimmerman, J. Criscione, J.W. Covell, Remodeling in myocardium adjacent to an infarction in the pig left ventricle, Am. J. Physiol. Heart Circ. Physiol. 287 (6) (2004) H2697–H2704.
[25] G. Abaqus, Abaqus 6.11, Dassault Systèmes Simulia Corp Providence, RI, USA, 2011.
[26] Y. Fung, What are the residual stresses doing in our blood vessels? Ann. Biomed. Eng. 19 (3) (1991) 237–249.
[27] J.M. Guccione, K.D. Costa, A.D. McCulloch, Finite element stress analysis of left ventricular mechanics in the beating dog heart, J. Biomech. 28 (10) (1995) 1167–1177.
[28] F. Scardulla, et al., Biomechanical determinants of right ventricular failure in pulmonary hypertension, Am. Soc. Artif. Intern. Organs J. 64 (4) (2018) 557–564.
[29] F. Scardulla, et al., Modeling right ventricle failure after continuous flow left ventricular assist device: a biventricular finite-element and lumped-parameter analysis, Cardiovasc. Eng. Technol. 9 (2018) 427–437.
[30] E. Berberoğlu, S. Göktepe, Computational modeling of myocardial infarction, Procedia IUTAM 12 (2015) 52–61.
[31] M. Sezer, et al., Infarct remodeling process during long-term follow-up after reperfused acute myocardial infarction, Am. J. Med. Sci. 338 (6) (2009) 465–469.
[32] M.S. Sirry, et al., Micro-structurally detailed model of a therapeutic hydrogel injectate in a rat biventricular cardiac geometry for computational simulations, Comput. Methods Biomech. Biomed. Eng. 18 (3) (2015) 325–331.
[33] F. Masithulela, Bi-ventricular finite element model of right ventricle overload in the healthy rat heart, Bio Med. Mater. Eng. 27 (5) (2016) 507–525.
[34] F. Masithulela, Analysis of passive filling with fibrotic myocardial infarction, in: ASME 2015 International Mechanical Engineering Congress and Exposition, American Society of Mechanical Engineers, 2015.
[35] R.C. Kerckhoffs, et al., Effects of biventricular pacing and scar size in a computational model of the failing heart with left bundle branch block, Med. Image Anal. 13 (2) (2009) 362–369.
[36] F.J. Masithulela, Computational biomechanics in the remodelling rat heart post myocardial infarction, in: Human Biology, University of Cape, Town: South Africa, Cape Town, 2016, p. 263.
[37] F. Masithulela, The effect of over-loaded right ventricle during passive filling in rat heart: a biventricular finite element model, in: ASME 2015 International Mechanical Engineering Congress and Exposition, American Society of Mechanical Engineers, 2015.
[38] E. Grandi, D. Dobrev, J. Heijman, Computational modeling: what does it tell us about atrial fibrillation therapy? Int. J. Cardiol. 287 (01) (2019) 155–161.
[39] M.A. Pfeffer, E. Braunwald, Ventricular remodeling after myocardial infarction. Experimental observations and clinical implications, Circulation 81 (4) (1990) 1161–1172.
[40] A. Martinsson, et al., Outcomes associated with dual antiplatelet therapy after myocardial infarction in patients with aortic stenosis, Int. J. Cardiol. 281 (2019) 140–145.
[41] F. Gungoren, et al., Optimal treatment modality for coexisting acute myocardial infarction and ischemic stroke, Am. J. Emerg. Med. 37 (4) (2019) 795. e1–795. e4.
[42] K. Kadner, et al., The beneficial effects of deferred delivery on the efficiency of hydrogel therapy post myocardial infarction, Biomaterials 33 (7) (2012) 2060–2066.
[43] T. Williams, et al., Missed acute myocardial infarction (MAMI) in a rural and regional setting, IJC Heart & Vasculature 22 (2019) 177–180.